RANS/LES COUPLING USING A FORCING TERM APPROACH

Younes Benarafa and Frédéric Ducros
CEA Grenoble
DEN/DER/SSTH/LMDL
17, rue des martyrs
38054 Grenoble cedex 9, France
younes.benarafa@cea.fr
frederic.ducros@cea.fr

Pierre Sagaut
LMM - UPMC/CNRS
Boite 162, 4 place Jussieu
75252 Paris cedex 05, France
sagaut@lmm.jussieu.fr

ABSTRACT

In nuclear industry the relevant flows are often wall bounded, characterized by a high Reynolds number turbulence and a strong unsteadiness. In order to develop an advanced numerical modeling that takes into account these features while extending on a large enough spatial flow configuration to be relevant for industrial goals, we start focusing on a methodology of coupling based on the following idea: we want to couple regions where standard fine resolved LES is used with regions resolved in the framework of RANS/LES coupling. This latter is considered here as full 3D unsteady simulations providing reasonable and accurate numerical solution with an affordable computational effort when compared to standard RANS modeling. The paper is devoted to this RANS/LES coupling method, based on the application of a forcing term and provides results on a first validation test on a fully and very coarse mesh. All the computations of this study were performed with the TRIO_U code developed at CEA (French Atomic Center) Grenoble. The RANS/LES coupling method applied in this study ensures a mean profile as correct as the RANS computation and an improvement for the fluctuations profiles compared to LES on coarse grid without forcing term.

INTRODUCTION

Industrial flow configurations concern most of the time turbulent, wall-bounded and high Reynolds number flows. For instance, the Reynolds number of a nuclear reactor pipe can be about one hundred million. Besides these flows exhibit strong anisotropic, transitional state, thermal effects and require a turbulence modeling as universal as possible. In that sense, Large Eddy Simulation (LES) seems to be a suitable approach to simulate such flows. However, in order to provide reliable results, LES may need a tremendous mesh refinement for the flows considered. If we consider the LES mesh requirements suggested by Baggett (1997) and the Dean correlation (assuming that it is suitable for a pipe flow configuration), the mesh requirement for the example above should be in order of one hundred billion of nodes. Such an important constraint is far beyond the reach of the nowadays computational power.

A first attempt to alleviate the computational cost of LES on wall-bounded flows consists in applying (more or less sophisticated) wall models to approximate the no-slip boundary condition. Nevertheless, even with the use of wall models, LES may provide spurious results on very coarse grids, see Nikitin et al. (2000), Nicoud et al. (2001) or Benarafa et al. (2005). Whereas RANS computations provide affordable and accurate mean results. From this point, the idea is to blend the Reynolds Averaged Navier-Stokes (RANS) approach and the LES techniques and to take benefit from the satisfying averaged RANS fields and the unsteadiness of the filtered LES quantities. The blending relies on a forcing term approach.

This study will be exposed in three parts. First, the numerical and the modeling framework will be unfolded. Then, the RANS/LES coupling method will be detailed. Finally, various results will be exposed and analyzed.

NUMERICAL SETUP AND MODELING FRAMEWORK

Governing equations and turbulence modeling

In this study the flow is incompressible and turbulent so that the mass conservation, the momentum filtered equations and the temperature transport equation can be expressed as follows :

$$\frac{\partial \overline{u}_j}{\partial x_j} = 0 \tag{1}$$

$$\frac{\partial \overline{u}_i}{\partial t} + \frac{\partial \overline{u}_i \overline{u}_j}{\partial x_j} = -\frac{1}{\rho}\frac{\partial \overline{P}}{\partial x_i} + 2\frac{\partial}{\partial x_j}\left((\nu + \nu_t)\overline{S}_{ij}\right) \tag{2}$$

$$\text{with} \quad \overline{S}_{ij} = \frac{1}{2}\left(\frac{\partial \overline{u}_i}{\partial x_j} + \frac{\partial \overline{u}_j}{\partial x_i}\right)$$

$$\frac{\partial \overline{T}_i}{\partial t} + \frac{\partial \overline{u}_i \overline{T}}{\partial x_j} = \frac{\partial}{\partial x_j}\left((\alpha + \alpha_t)\frac{\partial \overline{T}}{\partial x_j}\right) + Q \tag{3}$$

where $\overline{(.)}$ is a filter for a LES and a statistic average for a RANS computation. ν_t is either a subgrid-scale viscosity in the first case or a turbulent viscosity in the second case. ν is the molecular viscosity and α is the thermal diffusivity. Q is a heat source term to create heat flux in the channel flow.

As for the turbulence models, we used the selective structure function model (for more details about this subgrid-scale model, see Lesieur et al. (1996)) for the LES computations and the Jones and Launder k-ϵ model for the RANS computations. For both cases, the turbulent diffusivity α_t is determined assuming that the turbulent Prandtl number ($Pr_t = \frac{\nu_t}{\alpha_t}$) is considered as constant and is equal to 0.9, see Kawamura et al. (1998).

The flow configuration considered is well-known (see for example Moin et al. (1987) or Abe et al. (2001)) and consists in a bi-periodic channel flow developing in the x-direction (see Fig. 1). To deal with pressure loss induced by the friction effects and to ensure constant mass flow rate in the channel, a source term is added to the momentum equation (2) at each time steps.

The correlation of Dean (1978) is used to prescribe a friction Reynolds number Re_τ (based on the friction velocity u_τ, the half channel height h and ν) to the flow. It has to be noted that this correlation is only valid for a friction Reynolds number lying between 350 and 2.10^4.

Numerical setup

All the computations of this study were achieved with the TRIO_U code. This object oriented code solves equations (1) to (3) in a mixed finite volume/finite element approach for both structured and unstructured grids. For the present study, structured grids are considered ; unknowns are located in a staggered mesh and the discrete form of the equations is solved using a matrix projection scheme which is a derivative of the SOLA method originally developed by Hirt et al. (1975) (more details about this projection method are developed in Emonot (1992)).

Our study will focus on calculations carried out in structured (and staggered) grids. The divergence free constraint is ensured using a projection method : the Poisson's equation is solved using a Cholesky direct method.

Time advancement was ensured by a 3rd order Runge-Kutta explicit scheme. For the momentum equation (2), we use a centered 2nd order scheme for convection and diffusion terms. For the temperature transport equation (3), a centered 2nd order scheme and a QUICK scheme, as suggested in Chatelain et al. (2004), have been respectively used for the diffusive term and the convective term.

Wall model approach

As our meshes are very coarse, we used (i) for the velocity, a standard wall model based on the logarithmic law to determine the wall shear stress and (ii) for the temperature, a wall model relying on the Kader law (Kader, 1981) to correctly compute the wall heat flux. These two analytical laws can be expressed as follows :

$$\frac{U}{u_\tau} = \frac{1}{\chi} ln(y^+) + A \tag{4}$$

u_τ is the friction velocity defined as : $u_\tau = \sqrt{\frac{\tau_w}{\rho}}$. Where τ_w is the wall shear stress and ρ is the fluid density. This first formula is called the logarithmic law which is valid from a minimum distance of 30 wall units (one wall unit is equal to the ratio $\frac{u_\tau}{\nu}$) from the wall. A is a constant equal to 5.3.

$$\frac{T - T_w}{T_\tau} = Pr\, y^+ e^{-\Gamma} + [2.12\, ln[(1 + y^+)C] + \beta]e^{-1/\Gamma} \tag{5}$$

With :

$$\Gamma = \frac{10^{-2}(Pr\, y^+)^4}{1 + 5Pr^3 y^+} \quad \text{and} \quad C = \frac{1.5(2 - y/h)}{1 + 2(1 - y/h)^2}$$

In the second formula, the temperature is divided by the friction temperature T_τ which is defined as :

$$T_\tau = \frac{\alpha}{u_\tau} \left(\frac{\partial T}{\partial y}\right)_w \tag{6}$$

RANS/LES COUPLING METHOD

Many coupling methods between RANS and Large-Eddy Simulation are developed but very few concern the use of a forcing term. However, it seems that two independent teams tried that kind of approach at the same time (see Sergent (2002) and Schlüter et al. (2002)). We hereafter detail some features of Schlüter's paper.

Previous attempt.

Schlüter et al. (2002) investigated a similar approach using a virtual body force to generate outflow boundary conditions inside a gas turbine engine configuration. This body force f_i is added to the right hand side of the momentum equation (2) and it is applied in an overlapping region between a RANS region and a LES zone :

$$f_i = \frac{1}{\tau_f}(u_i^{RANS} - \widetilde{u}_i^{LES}) \tag{7}$$

The i-subscript corresponds to the velocity component and τ_f is the forcing time scale which was initially defined by the authors as the forcing region length divided by the bulk velocity. Schlüter and his co-authors also noted that this time scale definition should be considered as an upper limit. In this latter case, they explain that a right choice of a time averaging period δt is crucial because on the one hand, δt should be long enough so that $\widetilde{(.)}$ could be considered as a statistical average, on the other hand, δt should be short enough to allow to capture the low frequencies of the mean velocity field. They propose three versions of operator $\widetilde{(.)}$. The first one is the instantaneous velocity so that the body force damped almost completely the resolved turbulent fluctuations. Secondly, the $\widetilde{(.)}$ operator was an overall time averaging which avoids the fluctuations damping but does not allow unsteadiness for mean velocity field. The third one is an averaging over a trailing window.

Present forcing term formulation.

Whereas, Schlüter et al. (2002) used a forcing on a limited area of the flow configuration and with a constant time scale τ_f, we applied the forcing term on the entire computational domain and at each time steps.

The following body force $f_i^{rans/les}$ is added to the right hand side of the momentum equation (2) :

$$f_i^{rans/les} = W_i \, \frac{u_i^{rans} - u_i^{les}}{\Delta t} \quad \text{with} \quad W_i = \frac{|u_i^{rans}|}{||u^{rans}||} \tag{8}$$

W_i is a weight function so that the forcing term adapts to the intensity of the velocity component. u_i^{rans} is the i-component of the RANS velocity field and $||u^{rans}||$ is its local norm. Δt is the current time step. Moreover, a similar forcing term can be used for the temperature field :

$$f_T^{rans/les} = \frac{T^{rans} - \widetilde{T}^{les}}{\Delta t} \tag{9}$$

The major aim of these forcing terms is to make the averaged LES velocity field match RANS velocity field. The turbulent fluctuations resolved by the forced LES are damped unless the $\widetilde{(.)}$ operator is comparable to the statistic average of the RANS field. We investigate three types of filters applying on the instantaneous ϕ field (velocity or temperature) :
- A spatial (streamwise and spanwise) average (Spatial) :

$$\widetilde{\phi}(t, x_i) = \int\int_{x,z} \phi(t, x_i) \, dxdz \tag{10}$$

- An overall time average (OTA) :

$$\widetilde{\phi}(t, x_i) = \int_{t_{init}}^{t} \phi(\alpha, x_i) \, d\alpha \tag{11}$$

- The simple exponential smoothing (SES) :

$$\widetilde{\phi}(t, x_i) = \frac{\Delta t}{\tau} \, \phi(t, x_i) + \left(1 - \frac{\Delta t}{\tau}\right) \widetilde{\phi}(t - \Delta t, x_i) \tag{12}$$

The first filter is limited to the periodic plane channel flow since it requires two homogeneous flow directions. The second filter consists of a time average from the initial time (t_{init}) to the present time (t). As a third filter, we choose to use an approximation of the trailing time average. Indeed, to perform a significant statistic average over a time period, requires a tremendous memory storage of hundreds or thousands of complete fields, whereas the present filter requires to store only two fields. As the δt parameter used by Schlüter and his co-authors, τ is a time period which should be chosen long enough to average the turbulent fluctuations and short enough to render the possible unsteadiness of the mean flow.

RESULTS

All the computations have been performed in a channel flow configuration at friction Reynolds number equal to 10^4, on a coarse mesh since $(\Delta x^+, \Delta y^+, \Delta z^+)$ is equal to (2000, from 100 to 625, 1000). For computations with temperature transport, the Prandtl number is set to 0.71. All the profiles shown in this section are expressed in reduced values. The velocity is divided by the friction velocity u_τ and temperature is normalized by the friction temperature T_τ. All the statistics are computed from an instant when the flow is fully developed and during 80 channel turnovers. Table 1 is set to expose the various computations carried out in this study.

First, we will focus on the influence of the forcing term with the OTA filter on the velocity and the temperature fields. Secondly, the influence of each of the three filters used on the forcing term will be investigated. Besides, different values of the time parameter τ will be considered for the SES filter.

Table 1: Computations performed in this study.

Case	Simulation	Forcing term filter
Case 0	RANS+SWM	$\times$
Case 1	LES+SWM	$\times$
Case 2	Forced LES+SWM	Overall Time Average
Case 3	Forced LES+SWM	Spatial Average
Case 4	Forced LES+SWM	SES $\tau = 16$ turnovers
Case 5	Forced LES+SWM	SES $\tau = 120$ turnovers

Table 2: Error on the friction prediction compared with the RANS computation (Case 0).

Case	Case 1	Case 2	Case 3	Case 4	Case 5
$E(u_\tau)$	+12%	$< 1\%$	$< 1\%$	$\simeq 1\%$	$< 1\%$

Finally, the forcing term profiles and its influence through the balance stress will be analyzed.

Results for the velocity and the temperature field

In this subsection, we will focus on the forcing term results obtained with the OTA filter. As shown in Fig. 2, LES computation with a Standard Wall Model (LES+SWM) provides a mean velocity profile which is quite spurious since it does not match the logarithmic law. This typical phenomenon is symptomatic of a LES performed in a too coarse grid, see Nikitin et al. (2000), Nicoud et al. (2001) or Benarafa et al. (2005). However, the RANS (Case 0) and forced LES (Cases from 2 to 5) computations match completely which demonstrates that the forcing term succeeded to impose a correct mean behavior to the LES. To analyze the efficiency of the forcing term from the friction point of view, table 2 was established to compare the computed friction velocity with the one obtained with the RANS computation. Thus, the error on the friction prediction of a given Case n is estimated as follows :

$$E(u_\tau) = \frac{u_\tau^{\text{RANS}} - u_\tau^{\text{Case n}}}{u_\tau^{\text{RANS}}} \tag{13}$$

Table 2 demonstrates that the forcing term succeeded also to ensure that the friction is as satisfying as the RANS one, since $E(u_\tau)$ does not exceed 1%, whereas the coarse LES (Case 1) underestimates the friction velocity of 12 percents.

Let us now consider the velocity RMS fluctuations. Although, it is difficult to know the location and the level of the peak of streamwise velocity fluctuations for very high Reynolds numbers, it is commonly admitted that it is located at wall-distance of $y^+ = 15$ and that its level seem is constant $(2.7 - 2.8)$ with the increase of the Reynolds number, see Abe et al. (2001). In Fig. 3, the fluctuation peak is located at the second node ($y^+ \simeq 150$) whereas its level seem to be closer to the physical level for the forced LES. Near the channel center, the results are compared to the experiment of Comte-Bellot (1965) at a lower friction Reynolds number ($Re_\tau = 8160$). Case 1 seems to underestimate the value of the streamwise fluctuations which is increased in Fig. 3 by the friction shown before. As for the Forced LES, the level of the fluctuations is slightly overestimated. Nevertheless, a general trend is that

the RMS fluctuations of the LES with a forcing term seem to be improved given that the mean velocity field is corrected.

Now, to consider the influence of the forcing term on the temperature field, we applied the forcing term firstly only to the velocity field and then both to the velocity and to the passive scalar field. As for the velocity field, on Fig. 4 we can note that the temperature profile of LES+SWM present the same kind of behavior observed for the velocity field. Moreover, we can note that the velocity field forcing is not sufficient to make the mean temperature profile match the Kader law. This is probably due to the fact that the passive scalar field is obtained by different numerical schemes compared with the velocity field.

The same analysis can be done about the RMS fluctuations of temperature (Fig. 5). As for the velocity case we could not recover the physical position of the temperature fluctuation peak which is located at the same wall distance than velocity fluctuation peak according to Subramanian and Antonia (1981). These authors also demonstrate that the intensity of the peak is constant with the Reynolds number. Moreover, according to these authors, the normalized temperature peak is about 2.0 respectively to the Prandtl number considered in the present study. This latter result shows that the prediction of the intensity of the peak seem to be better in the cases with a forcing term.

Filter influence on the present result

We will now discuss the influence of the filter $\widetilde{(.)}$ used in the forcing term (8). The overall time averaging (Case 2), the simple exponential smoothing when the τ parameter is high enough (Case 5) and the spatial average (Case 3) seem to provide similar results as for the mean profiles as for RMS fluctuations. However, the τ parameter of the SES filter appeared to be quite sensitive. Actually, this point has been developed by Schlüter (2002), if τ is too short the trailing time average tends to the instantaneous value and then, the forcing term damps the velocity high frequencies since it forces a part of the instantaneous signal to match the RANS signal which concerns low frequencies. The effects of a too small value of τ is not very strong if we consider only the mean profiles, whereas they can clearly be noticed on the RMS fluctuations profiles. In fact, when τ corresponds to 16 channel turnovers, the RMS velocity fluctuations (Fig. 3) are clearly lowered comparing with the Case 5, in which τ corresponds to 120 channel turnovers. In this latter case, the SES filter and the OTA filter have similar results. These identical behaviors can be observed when τ is higher than 80 channel turnovers.

Forcing term profiles and balance stress

To carry on the analysis of the mechanisms implied by a forcing term on the momentum equation, we will observe the forcing term profiles and the balance stress. Focusing on Fig. 6, we note that the mean forcing term is very small but not equal to zero which shows that it is active all along the computation. Its maximum is located at the first computation node correcting this way the wall shear stress. Moreover, the RMS forcing term profile indicates that it highly fluctuates, especially at the first computation nodes.

To evaluate the influence of the forcing term on the flow, the balance stress of computations with a forcing term is analyzed. With the use of this latter, the stress balance can be written as follows :

$$\underbrace{-\frac{\langle u'v'\rangle}{u_\tau^2}}_{(A)} + \underbrace{\langle\frac{\partial U^+}{\partial y^+}\rangle}_{(B)} + \underbrace{\langle\frac{\nu_t}{\nu}\frac{\partial U^+}{\partial y^+}\rangle}_{(C)} \underbrace{-\langle f\rangle\frac{\nu}{u_\tau^3}y^+}_{(D)} = 1 - \frac{y^+}{Re_\tau} \quad (14)$$

The classical balance stress in a plane channel flow is retrieved with the Reynolds stress (A), the viscous stress (B) and the modeled stress (C), but the contribution of the forcing term is added (D). This balance is set in Fig. 8 for the OTA filter (it is recalled that the SES filter with τ equal to 120 turnovers provides very similar results to the OTA filter) and in Fig. 9 for the SES filter ($\tau = 16$ turnovers) and it is compared with the balance of the coarse LES+SWM (see Fig. 7). In this latter figure, the LES+SWM exhibits a very high total shear stress $((A)+(B)+(C)-(D))$ near the second node which is probably due, as discussed before, to unphysical large streaks typically encountered in coarse mesh LES. In this case, if the total shear stress does not meet, for the near wall computational nodes, the theoretical balance (right hand side of (14)), it is due to the fact that numerical errors implied by the coarseness of the grid are not negligible.

As for the forced LES (Fig. 8 and Fig. 9), the additional term (D) (called *force stress*) appears to be negligible compared with other stresses. Nevertheless, the Reynolds stress for the OTA filter (Fig. 8) shows a surplus which indicates that the forcing term has an influence on the results. This surplus appears from the fourth computational node which corroborates the fact that the fluctuations level is higher from the same distance to the wall for the forcing term computation (see Fig. 3). The Reynolds stress surplus is due to a higher level of the production of the turbulent kinetic energy (not shown here) which becomes, thanks to the forcing term approach, less sensitive to numerical errors implied by the coarse grid.

As for the forcing term with the SES filter (Fig. 9), the Reynolds stresses are drastically damped as it could be expected before, given the behavior of the fluctuations. This result suggests that it should be possible to find a tricky value of τ for the SES filter which would allow the forcing term approach to ensure a correct mean profile and wall shear stress without implying necessarily a surplus of turbulence production.

CONCLUSION

In this study, we carried out several unsteady computations at really high Reynolds number on coarse grids thanks to the TRIO_U code. First, several drawbacks have been found out for large-eddy simulations even with the use of wall models. Then, a forcing term RANS/LES approach was used to avoid some of these drawbacks as a spurious mean profile or as an underestimation of the wall shear stress. The presented results show that correcting efficiently the passive scalar field implies the use of an additional forcing term applied on this field.

Besides, the filter applied to the LES field in the forcing term appear to be an important parameter. The spatial filter and the overall time averaging perform a satisfying forcing on the mean field and eliminate the spurious streaky structures typical of coarse meshes. As for the simple exponential smoothing, it implies a fluctuations damping if the τ parameter is smaller than 80 channel turnovers.

It was also noted that the computations with a forcing

term presented a significant Reynolds stress surplus. This phenomenon is due to an increase of the turbulence production inherent in the forcing term approach. A possible remedy would be to choose carefully the τ parameter in SES filter to impose a satisfying mean profiles and wall shear stress and to avoid a surplus of turbulence production.

REFERENCES

Abe, H., Kawamura, H., and Matsuo, Y., 2001, "Direct Numerical Simulation of a fully developed turbulent channel flow with respect to Reynolds number dependence", *Journal of fluids engineering*, Vol. 123, pp 382-392.

Baggett, J. S., 1997, "Resolution requirements in large-eddy simulations of shear flows", *Annual Research Briefs - Center for Turbulence Research*, pp 51-66.

Benarafa, Y., Cioni, O., Ducros, F., and Sagaut, P., 2005, "RANS/LES coupling for unsteady turbulent flow simulation at high Reynolds number on coarse meshes", *Computer Methods in Applied Mechanics and Engineering*, In Press.

Châtelain, A., Ducros, F., and Métais, O., 2004, "LES of heat transfert : proper numerical schemes for temperature transport", *Int. J. Numer. Meth. Fluids*, Vol. 44, pp 1017-1044.

Comte-Bellot, G., 1965, "Ecoulement turbulent entre deux paroi parallles", *Publications Scientifiques et Techniques du Ministre de l'Air no. 419*, (*In French*).

Emonot, P., 1992, "Méthodes de Volumes Elements Finis : Application aux équations de Navier-Stokes et résultats de convergence", *PhD thesis, Université Claude Bernard - Lyon I*, (*In French*).

Hirt, C. V., Nichols, B. D., and Romero, N. C., 1975, "SOLA - a numerical solution algorithm for transient flow", *Los Alamos National Laboratory, Report LA-5852.*

Kader, B. A., 1981, "Temperature and concentration profiles in fully turbulent boundary layers", *Int. J. Heat Mass Transfer*, Vol. 24, pp 1541-1544.

Kasagi, N., Tomita, Y., and Kuroda, A., 1992, "Direct Numerical Simulation of passive scalar field in a turbulent channel flow", *ASME J. Heat Transfer*, Vol. 114, pp 598-606.

Kawamura, H., Ohsaka, K., Abe, H., and Yamamoto, K., 1998, "DNS of turbulent heat transfer in channel flow with low to medium-high Prandtl number fluid", *Int. J. Heat and Fluid Flow*, Vol. 19, pp 482-491.

Kim, J., Moin, P., and Moser, R., 1987, "Turbulence statistics in fully developed channel flow at low Reynolds number" *J. Fluid Mech.*, Vol. 177, pp 133-166

Lesieur, M., and Métais, O., 1996, "New trends in large-eddy simulations of turbulence", *Ann. Rev. Fluid. Mech.*, Vol. 28, pp 45-82.

Nikitin, N. V., Nicoud, F., Wasistho, B., and Squires, K. D., 2000, "An approach to wall modeling in large-eddy simulations", *Physics of Fluids*, Vol. 12, No 7, pp 1629-1632.

Nicoud, F., Baggett, J. S., Moin, P., and Cabot, W., 2001, "Large eddy simulation wall-modelling based on suboptimal control theory and linear stochastic estimation", *Physics of Fluids*, Vol. 13, No 10, pp 2968-2984.

Schlüter, J. U., Pitsch, H., and Moin, P., 2002, *AIAA Paper*, No 3121.

Sergent, E., 2002, "Vers une méthodologie de couplage entre la Simulation des Grandes Echelles et les modèles statistiques", *PhD thesis - Ecole Centrale de Lyon*, (*In French*).

Subramanian, C. S., and Antonia R. A., 1981, "Effect of the Reynolds number on a slightly heated turbulent boundary layer", *Int. J. Heat Mass Transfer*, Vol. 24, No 11, pp 1833-1846

FIGURES

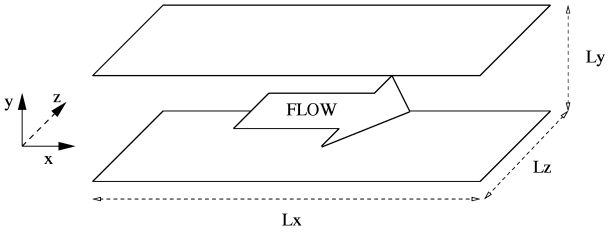

Figure 1: Plane channel flow.

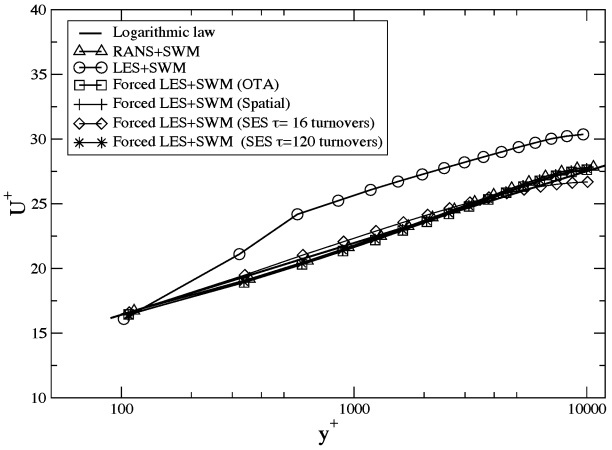

Figure 2: Reduced mean streamwise velocity profiles.

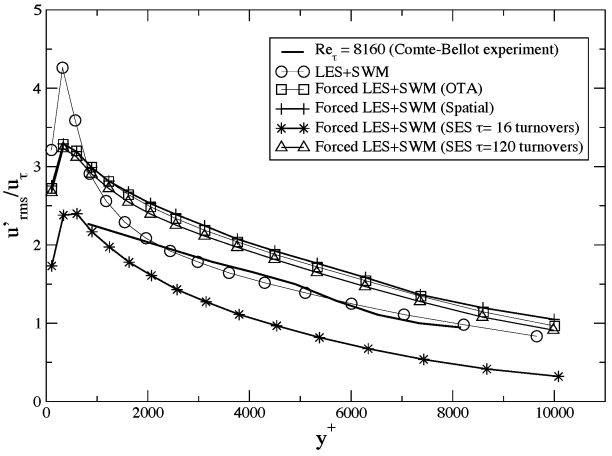

Figure 3: Reduced RMS streamwise velocity fluctuations profiles.

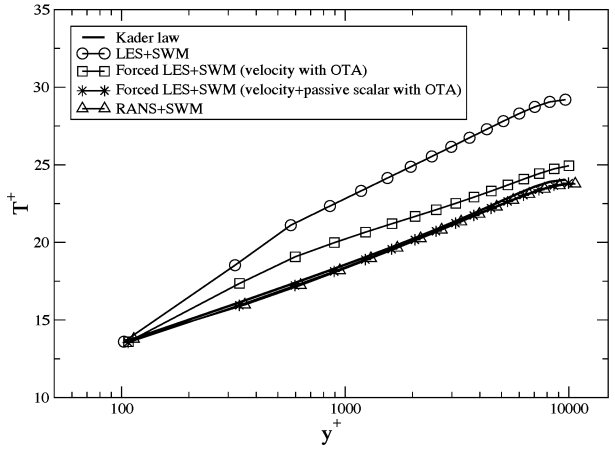

Figure 4: Reduced mean temperature profiles.

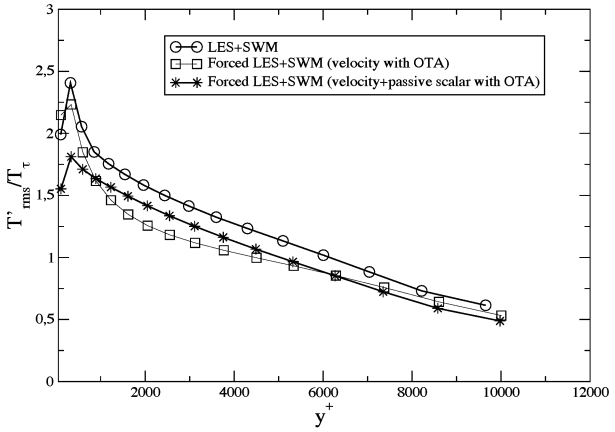

Figure 5: Reduced RMS temperature fluctuations profiles.

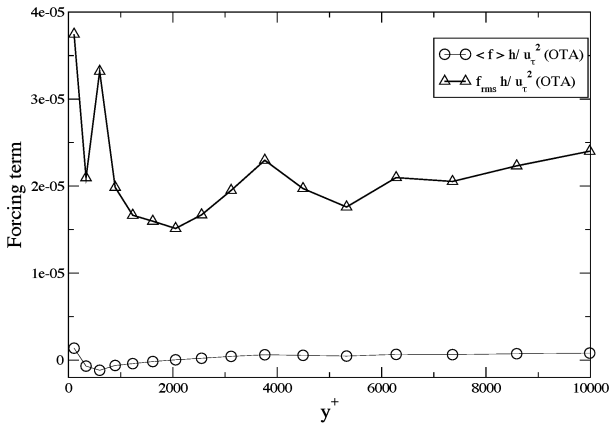

Figure 6: Reduced mean and RMS forcing term profiles.

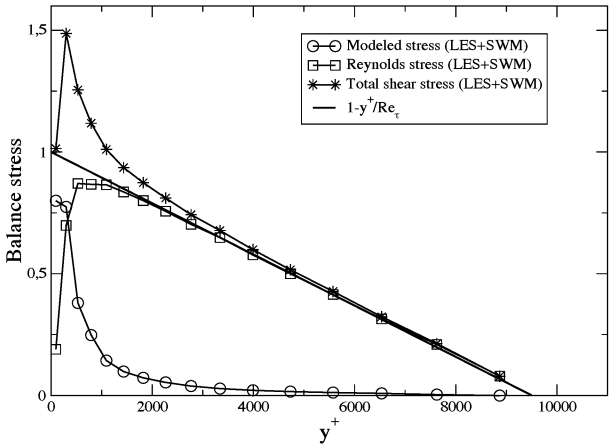

Figure 7: Balance stress profiles for the coarse LES+SWM (Case 1).

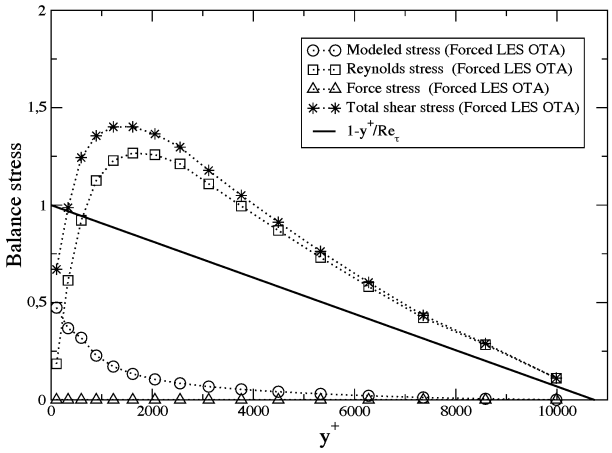

Figure 8: Balance stress profiles for the Forced LES with OTA filter (Case 2).

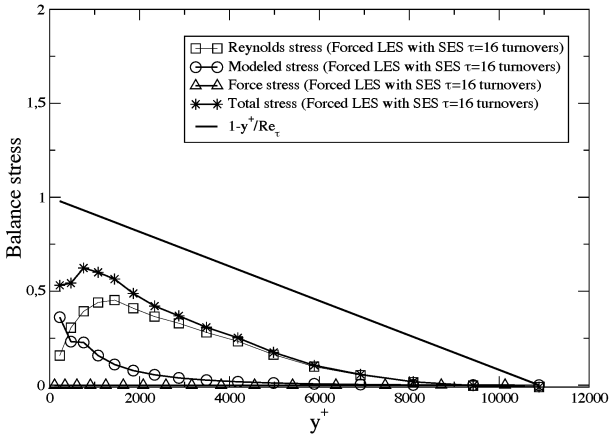

Figure 9: Balance stress profiles for the Forced LES with SES filter ($\tau = 16$ turnovers) (Case 4).